FATIGUE BEHAVIOR OF A 3D BRAIDED CARBON/EPOXY COMPOSITE

V. Carvelli[1]*, J. Pazmino[1], S.V. Lomov[2], A.E. Bogdanovich[3],
D.D. Mungalov[3], I. Verpoest[2]
[1] Department of Structural Engineering, Politecnico di Milano, Italy
[2] Department of Metallurgy and Materials Engineering, K. U. Leuven, Belgium
[3] 3TEX Inc., Cary NC, USA
* Corresponding author (valter.carvelli@polimi.it)

Keywords: *3D braided composite, Fatigue life, Fatigue damages*

1 Introduction

Three-dimensional (3D) braided unitary fabrics have a number of distinct features in their architecture and some important advantages over prepreg tape laminates and other types of 2D and 3D fabric used as preforms for composites ([1], [2]). They provide high conformability and drapability, suppression of delamination owed to the presence of through thickness reinforcement, improved damage tolerance, impact resistance, shear stiffness and strength, and increased torsional rigidity. The advanced, automated computer controlled technology (like the recent novel 3D rotary braiding process and machines developed by 3TEX, Inc., see Fig. 1 and further information in [3], [4]) provides efficient and affordable manufacturing means for producing complex shape fabric preforms for composites. The broad range of applications of 3D braided composites in the aerospace, marine, automotive, infrastructure and other industries ([5], [6]) require an in-depth knowledge of their mechanical properties. In the authors' knowledge, publications dealing with experimental studies of the fatigue behavior of 3D braided carbon fiber composites are not available in literature. This is the main topic of the present work.

The fatigue experimental investigation, detailed in this paper, involved:

- tensile-tensile cyclic tests for different stress levels in the longitudinal direction, in order to obtain a fatigue life curve of the material;
- tensile-tensile cyclic tests of 3D braided carbon composites with different V_f to evaluate the effect of the fiber volume fraction (V_f) on the fatigue life;
- micro-CT observations of the material after different number of cycles to capture the evolution of the damage imparted during the cyclic lading.

Besides the aforementioned experimental work, other mechanical tests and experimental observations (not included in this paper but to be presented at the Conference) were performed. Those are:

– the observation and measurement of the internal shape of the yarns inside the composite by microscopy and micro-CT images;
– the assessment of the quality of impregnation by micro-CT three-dimensional observation of voids inside the composite;
– the pre-fatigue quasi-static tensile tests in the longitudinal (braiding) direction of the reinforcement with acoustic emission recording and strain mapping by DIC technique to detect the initiation and development of the damage;
– the post-fatigue quasi-static tensile tests of specimens cyclically loaded for different number of cycles aimed at understanding of the influence on the mechanical properties upon the damage imparted during the fatigue loading.

2 Material Features

The fabric is made of Toho Tenax 12K HTS carbon yarns. The preform material was produced on the 144-horngear, 576-carrier 3D rotary braider at 3TEX, Inc. (Fig. 1). The manufacturing of 3D braided preform, having rectangular cross section, involved the total of 96 fiber carriers and the braiding pattern shown in Fig. 2. Fig. 3 illustrates fiber architecture of the 3D braid. Linear weight of the fabric is 78.8 ± 0.5 g/m.

The braided composite samples were produced entirely at room temperature. The preform was first soaked with Epoxy West System 105 resin (209

hardener) and then placed in a special, 3TEX constructed [5], pressure mold with open ends aimed at releasing excess of resin and air bubbles when the soaked preform is pressurized. The preform was kept in the mold under step-wise increasing pressure for the resin gelling time 50 min. After that the preform stayed in the mold for several hours at constant pressure to allow the resin to fully cure. Then the produced composite in the form of bars having 50 cm length and 25.4 mm width were released from the mold. No post-cure was applied.

Fig. 1. 3D rotary braiding machine at 3TEX, Inc. with full 576-carrier fiber set up and axial fiber supply from the creel.

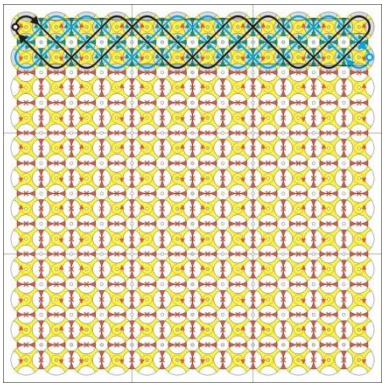

Fig. 2. 3D braiding pattern utilized for the rectangular cross section preform fabrication.

The first batch of material produced for this study had V_f within the composite samples of 55.6% ± 0.4%. The void content was measured in the range between 0.8% and 2.3% with average 1.5%. The angle between the braiding yarns has been measured on the surface of the composite samples, and it appeared to be 10.0° ± 0.5°. This angle is different from the true braid angle inside the manufactured preform (defined as the angle between braided fiber direction and the braid formation direction); the latter angle was evaluated as 14°.

Other batches of the same material have been produced, using the above described process. In those samples, only the thickness of the composite (the V_f value, respectively) has been varied. This allowed for investigating the influence of the fiber volume fraction on the mechanical properties of the composite. Table 1 presents the V_f values of the investigated materials along with the measured average thickness and porosity.

The fabricated 3D braided composite bars were cut along the length into test specimens for tension and fatigue testing; each specimen was 25 cm long.

Fig. 3. Fiber architecture of the produced 3D braided preform.

V_f %	**Thickness [mm]**	**Porosity %**
47.9	3.68	1.64
51.6	3.40	2.45
55.6	3.21	1.50
58.4	3.01	1.95
63.2	2.79	2.12

Table 1. Fiber volume fraction (V_f), thickness and porosity of the braided composite bars.

3 Tensile-tensile cyclic tests

The response to fatigue loading of the 3D braided carbon/epoxy composite was investigated by means of tension-tension cyclic tests.

The aim of the fatigue tests are: (i) to obtain the stress level at which complete failure did not occur before 5 million cycles (σ_{5m}); (ii) to produce the fatigue life curve (σ-N) of the material with V_f = 55.6%; (iii) to compare the fatigue life of the braided composite with different fiber volume fractions (section 4); (iv) to observe the damage imparted during the cyclic loading (section 5).

Aluminum tabs, 70÷80 mm long and 2 mm thick, were used to grip the specimen in two hydraulic MTS testing machines. Tests were performed under constant stress amplitude, sinusoidal wave-form tensile-tensile loading with the ratio R = 0.1 (ratio of the minimum to the maximum stress in the cycle). The stress was evaluated by using the sample cross-sectional area averaged from three measurements. The frequency was set to 6 Hz.

The fatigue tests of composite V_f = 55.6% involved different maximum stress (σ_{max}) levels in the cycle, ranging from 950 MPa (the respective average static strength is 1351 MPa) to the stress level at which complete failure did not occur before 5 million cycles (σ_{5m}). The complete specimen failure means that it separated into two parts during cyclic loading (as illustrated in Fig. 4). At least three valid tests have been performed for each stress level. A cyclic test was considered ‘‘valid” if the specimen did not break in the tabs, or close to the tabs. This requirement was not satisfied for the cyclic tests involving stress levels higher than 950 MPa.

Fig. 4. Fatigue failure of a specimen.

The response to cyclic tensile loading at different stress levels allowed us to determine the stress level σ_{5m} as 800 MPa for V_f = 55.6%.

Some information on the behavior of the composite material during the cyclic loading was extracted from the observed variation of the shape of the fatigue stress–displacement cycles during the test. The upper part of the plot in Fig. 5 shows the comparison of some cycle curves of the specimen loaded with a maximum stress of 800 MPa (e.g. the stress level defined as σ_{5m}). The slope of the cycle curve segment passing through the points of maximum and minimum stress (‘‘cycle slope”) continuously decreases up to 3 million cycles, as seen in Fig. 5. Above 3 million cycles, the slope remains nearly constant. These observations are further confirmed by observing the evolution of the maximum and minimum displacements under increasing number of cycles (see the lower diagram in Fig. 5). The reduction of the cycle slope within initial 3 million cycles suggests that there is some stiffness degradation of the material caused by the damage accumulation during cycling.

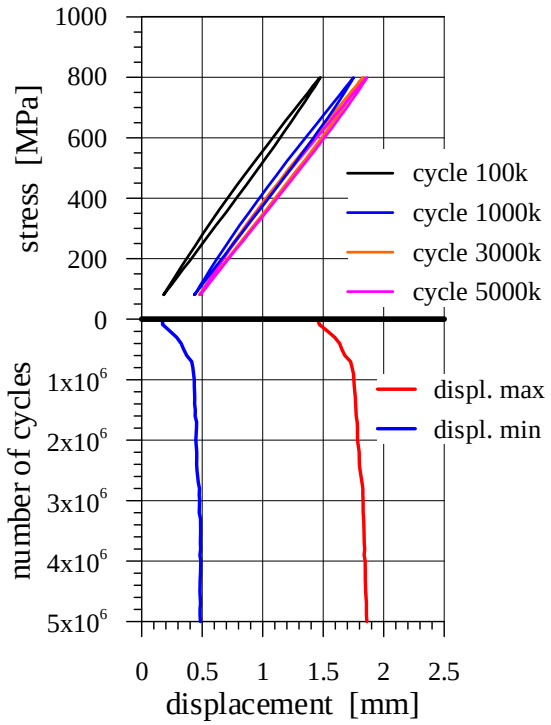

Fig. 5. Cyclic test with maximum stress 800 MPa. Some stress vs. displacement curves; maximum and minimum displacement vs. number of cycles for a specimen of V_f = 55.6%.

Differently, the evolution of the damage reflects in a continuous decrease of the material stiffness if the maximum stress is 850 MPa. The specimen fatigued with this stress level shows continuous decrease of the cycle slope (respectively, continuous decrease of the stiffness), as depicted in Fig. 6. The increasing hysteresis area of the cycles and the increase of the recorded maximum and minimum displacements (as seen in Fig. 6) demonstrate a gradual damage development, leading to the ultimate failure of the specimen.

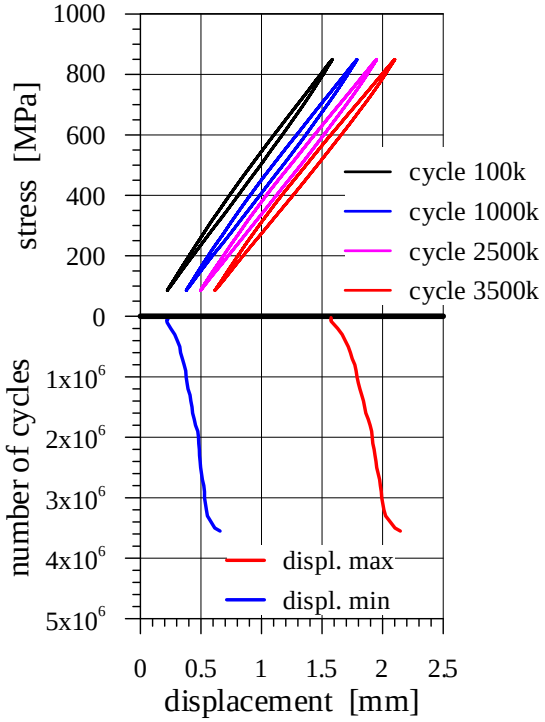

Fig. 6. Cyclic test with maximum stress 850 MPa. Some stress vs. displacement curves; maximum and minimum displacement vs. number of cycles for a specimen of V_f = 55.6%.

The fatigue tests performed in the considered stress range enable for depicting a fatigue life curve (Wöhler-type diagram) for the braided composite with V_f = 55.6%. In Fig. 7, the valid tests of the composite are represented by the maximum stress in the cycle (σ_{max}) vs. the number of cycles to failure N. In the diagram, the average static tensile strength is also indicated in its correspondence to the extrapolated lowest number of cycles, N=1.

Appropriate fitting equation was applied to the obtained experimental fatigue data. It enables for reliable predictions of the fatigue life corresponding to the other stress levels, which were not investigated in the present experimental study. The diagram in Fig. 7 shows the fitting of obtained experimental results (run-outs are not included) by means of a linear segment. The semi-logarithmic function adopted is $\sigma_{max} = a\, logN + b$, where a and b are –34.6 and 1351, respectively.
The quality of the fitting is related to the coefficient of correlation R^2 [7]. Values of R^2 close to 1 confirm the reliability of the fitting. The curve in Fig. 7 has a coefficient of correlation of 0.998.

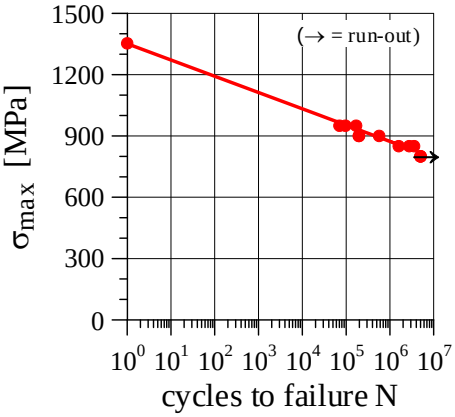

Fig. 7. Fatigue life curve of the 3D braided carbon fiber composite (V_f = 55.6%).

4 Fatigue life vs. fiber volume fraction

The effect of the fiber volume fraction on the fatigue life of the 3D braided composite materials was investigated on test specimens having five different V_f values (see Table 1). A reduced number of specimens have been produced for composites having V_f higher and lower than 55.6%. This set of cyclic tests was not performed for all of the maximum stress levels used for the specimens with V_f = 55.6%.
The results of the cyclic tests of the composite materials with different V_f are collected in the diagram of Fig. 8 as the average number of cycles to failure vs. the maximum stress in the cycle (σ_{max}).
The histogram in Fig. 8 shows that:

- increasing the V_f value results in the increase of stress level σ_{5m};
- increasing the V_f value for each maximum stress level results in the increase of the fatigue life.

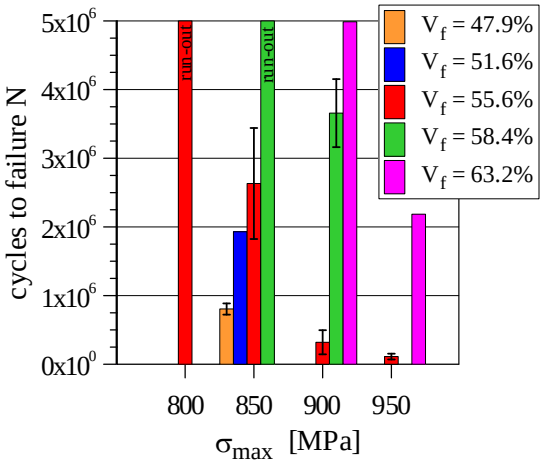

Fig. 8. Fatigue life of the 3D braided carbon fiber composite with different V_f values.

5 Fatigue damage observations

The damage development during tensile-tensile fatigue tests has been investigated by means of X-ray micro-computed tomography (micro-CT) observations of the cross sections of the damaged specimens (see [8], [9] for details of this experimental technique).

A Philips HOMX 161 X-ray system (Philips X-ray, Germany) with the AEA Tomohawk upgrade (AEA Technology, UK) was used for micro-CT images acquisition. Its detector system has an image intensifier TH 9428HX and a CCD camera (1024x1024 pixels) 12 bit dynamic range. An angular increment of 0.3 degree was adopted.

Tensile-tensile fatigue tests with accompanied damage observation have been performed for the composite material loaded with maximum stress level σ_{5m}, which was assessed as 800 MPa for the materials with for $V_f = 55.6\%$. The fatigued specimens have been observed after 1 and 3 million cycles. Three zones along the free edge of the specimen have been monitored.

In Fig. 9 and Fig. 10 the same part of the specimen is reproduced after 1 and 3 million cycles, respectively. In both figures the top picture represents the cross section of the specimen, while the three bottom pictures represent: (a) the front view in the length-width plane of the specimen; (b) cross-sectional view in the width-thickness plane; (c) lateral view in the length-thickness plane.

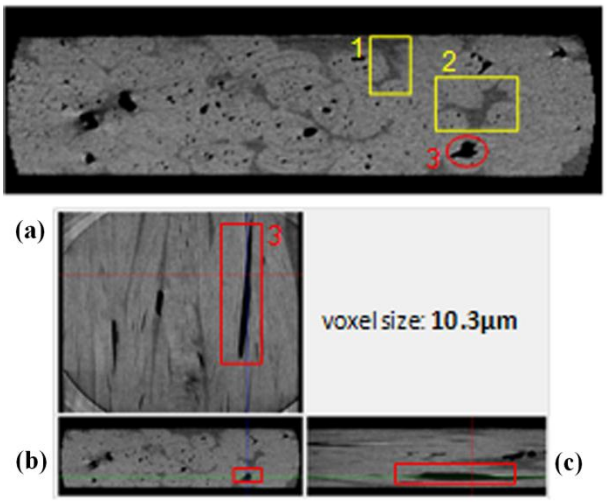

Fig. 9. Damage imparted after 1 million cycles for a maximum stress in the cycle of 800 MPa.

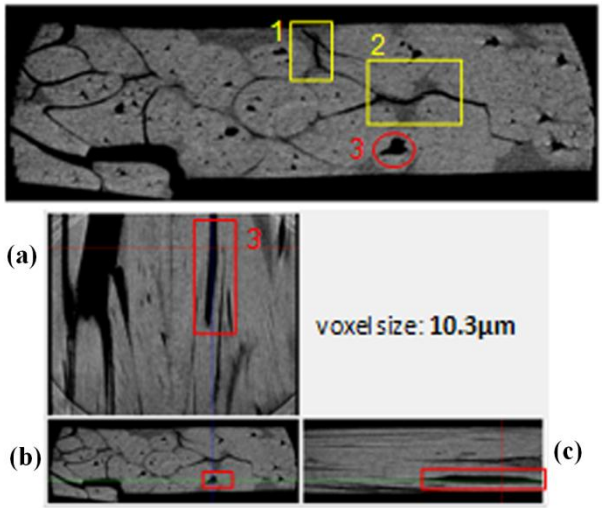

Fig. 10. Damage imparted after 3 million cycles for a maximum stress in the cycle of 800 MPa.

A qualitative comparison of the pictures show some cracks appearing during the first million cycles; those do not develop with increasing number of cycles (see the one named 3 in Fig. 9 and Fig. 10). Other cracks, not visible in Fig. 9, initiate and

develop for a number of cycles higher than 1 million (see those in the regions named 1 and 2). The observed cracks seem to be originated in the resin rich zones; then they develop along the matrix-yarn interfaces. The mechanism on the damage development extracted from the diagram in Fig. 5 seems to be confirmed by the analysis of the micro-CT pictures. The damage initiates and develops within 3 million cycles, when the stiffness degradation of the material is mainly observed, and does not show further increase that may lead to a complete failure before 5 million cycles.

It should be emphasized that the specimen used for the micro-CT observations during the cyclic loading failed several thousands of cycles prior to the 5 million cycle loading mark, even though the applied maximum stress was σ_{5m}. This result allows one to suggest that the observed damage state in that particular specimen was more critical than the damage states in all those specimens which did not failed under the same applied stress level.

6 Conclusions

A comprehensive experimental study presented in this paper characterizes the tensile-tensile fatigue behavior of one representative composite material reinforced with 3D braided carbon fiber fabric. Results of the performed fatigue tests show that:

- the stress level at which complete fatigue failure of the composite with $V_f = 55.6\%$ did not occur before 5 million cycles, is close to 60% of the respective static strength limit;
- the fatigue life increases with increasing fiber volume fraction in 3D composite;
- the damage observed by micro-CT of the specimens tested up to 3 million cycles for $\sigma_{max} = \sigma_{5m}$, is initiated in the resin rich zones between the yarns and further develops along the yarn-matrix interfaces.

References

[1] L. Tong, A.P. Mouritz, M.K. Bannister, "*3D fibre reinforced polymer composites*", Elsevier, 2002.

[2] A.E. Bogdanovich and M.H. Mohamed, "Three-Dimensional Reinforcements for Composites". *SAMPE Journal*, vol. 45, No. 6, pp. 8-28, 2009.

[3] D. Mungalov and A. Bogdanovich, "Automated 3-D Braiding Machine and Method". US Patent No. 6,439,096 B1, issued August 27, 2002.

[4] A. Bogdanovich, D. Mungalov, "An overview of recent advantages in 3D rotary braiding technology". *Proceedings 48th SAMPE-USA Symposium*, Long Beach, USA, pp. 1264-1278, 2003.

[5] D. Mungalov and A. Bogdanovich, "Complex Shape 3-D Braided Composite Preforms: Structural Shapes for Marine and Aerospace". *SAMPE Journal*, vol. 40, No. 3, pp. 7-20, 2004.

[6] D. Mungalov, P. Duke, A. Bogdanovich, "High Performance 3-D Braided Fiber Preforms: Design and Manufacturing Advancements for Complex Composite Structures". *SAMPE Journal*, vol. 43, pp. 53-60, 2007.

[7] L.J. Bain, M. Englehardt, "*Introduction to probability and mathematical statistics*". 2nd edition, Duxbury Press, 2000.

[8] S.V. Lomov, D.S. Ivanov, T.C. Truong, I. Verpoest, F. Baudry, K. Vanden Bosche, H. Xie, "Experimental methodology of study of damage initiation and development in textile composites in uniaxial tensile test". *Composites Science and Technology*, vol. 68, pp. 2340-2349, 2008.

[9] P.J. Schilling, B.R. Karedla, A.K. Tatiparthi, M.A. Verges, P.D. Herrington, "X-ray computed microtomography of internal damage in fiber reinforced polymer matrix composites". *Composites Science and Technology*, vol. 65, pp. 2071-2078, 2005.